Precision Microwave Measurement of the Internal Parasitics of Tunnel-Diodes

J. W. BANDLER, MEMBER, IEEE

Abstract—**This paper reports the results of precision microwave standing-wave measurements using a superheterodyne technique from 4 to 11 GHz on the internal parasitics of tunnel-diodes terminating a coaxial-line. Because of past conflicting conjectures as to the frequency dependence of the series resistance, particular attention has been paid to its accurate evaluation. Errors due to transmission-line attenuation and mount discontinuities have been explicitly eliminated from the measured results. The frequency invariance of the series inductance and junction capacitance is verified; but a new variation of series resistance with frequency is proposed of the form $r=r_{dc}+(af)^2$, in accordance with the experimental results. The effect of this variation on the resistive cutoff frequency is discussed and a comparison is made with the relevant results of other researchers.**

I. Introduction

The variation with frequency of the parameters of the equivalent circuit of the tunnel-diode is of some concern to designers of tunnel-diode circuits, especially at microwave frequencies. In the absence of conclusive measurement results indicating the contrary, the parameter values measured mainly at dc are usually assumed to be valid. After studying the papers concerned with the microwave measurement of tunnel-diode parameters,[1]–[6] one must come to the conclusion that all parameters except the series resistance are substantially constant within experimental error, at least as far as X-band. This series resistance is an elusive parameter, particularly when it has a low value. It is not surprising, therefore, that different experimenters have observed different apparent variations of this parameter at microwave frequencies.

This paper presents the results of what are believed to be the most precise microwave standing-wave measurements reported to date on the tunnel-diode biased at its valley voltage. The series resistance, series inductance, and junction capacitance, i.e., all the "internal" parasitics, are evaluated for this bias condition. The measurements were carried out on a specially fabricated coaxial-line mount containing the tunnel-diode. The mount was connected to a precision slotted-line through a precision connector. The superheterodyne technique was used for obtaining greater sensitivity at the low power levels required, with the source connected to the probe. The frequency range 4 to 11 GHz was covered.

Manuscript received November 28, 1967; revised February 9, 1968. The results of this paper were presented at the IEEE International Electron Devices Meeting, Washington, D. C., October 18–20, 1967. This work was carried out by the author at Mullard Research Laboratories, Redhill, Surrey, England.

The author is with the Department of Electrical Engineering, University of Manitoba, Winnipeg, Canada.

Reactive effects attributed to the discontinuity between the coaxial-line and the tunnel-diode package were measured and taken account of. The effect of attenuation along the transmission-line was considered both theoretically and experimentally and is also eliminated from the measurements.

II. Transmission-Line with Small Finite Attenuation

Attenuation is a fundamental limitation to the accurate measurement of VSWR at a transmission-line load. Fig. 1 illustrates the situation.

Approximate Equivalent Circuit

It is well known that a resistance ladder network can represent a section of lossy transmission-line. If the attenuation is small, the L section of Fig. 1(b) at the load is sufficiently accurate. r_s, r_p, and z_L are normalized to the line's characteristic impedance. ρ_L and ρ are the reflection coefficients at the load and input terminals, respectively, in Fig. 1(a), and ρ' and ρ'' the corresponding quantities in Fig. 1(b). For Fig. 1(a),

$$\rho = \rho_L e^{-2\alpha l} e^{-2j\beta l}. \tag{1}$$

Let the equivalent normalized load impedance in Fig. 1(b) be z. When $z_L=0$, $z=r_s$; when $z_L=\infty$, $z=r_s+r_p$. $|\rho''|=|\rho|$ for these cases if

$$\frac{1}{r_s} = \frac{r_s + r_p}{1} = s_0 \tag{2}$$

where s_0 is the corresponding VSWR. Now, in general,

$$\rho' = \frac{r_s r_p + r_s z_L + r_p z_L - r_p - z_L}{r_s r_p + r_s z_L + r_p z_L + r_p + z_L}. \tag{3}$$

Let s_0 be fairly large, say $s_0 > 10$ (a condition satisfied in the present work), then

$$\frac{r_s + r_p}{r_s} = s_0^2 > 100.$$

Therefore,

$$r_p \gg r_s \tag{4}$$

and

$$r_s r_p \simeq 1. \tag{5}$$

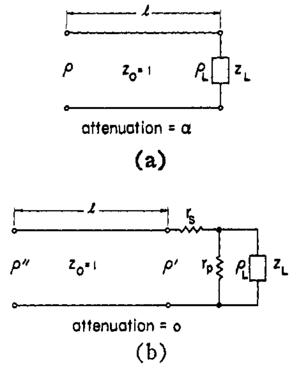

Fig. 1. Lossy transmission-line. (a) Conventional representation. (b) Approximate equivalent circuit for small attenuation.

This reduces (3) to

$$\rho' \simeq \frac{1 + r_p z_L - r_p - z_L}{1 + r_p z_L + r_p + z_L} = \frac{(z_L - 1)(r_p - 1)}{(z_L + 1)(r_p + 1)} \simeq \rho_L \frac{s_0 - 1}{s_0 + 1}. \tag{6}$$

Therefore,

$$\rho'' = \rho' e^{-2j\beta l} \simeq \rho_L \frac{s_0 - 1}{s_0 + 1} e^{-2j\beta l}. \tag{7}$$

Also, from (1) and (7),

$$e^{-2\alpha l} \simeq \frac{s_0 - 1}{s_0 + 1} \simeq 1 - \frac{2}{s_0}$$

giving

$$\alpha l \simeq \frac{1}{s_0} \text{ nepers.} \tag{8}$$

Since s_0 is independently defined, (8) does not actually depend on the equivalent circuit.

Suppose $|z_L| \ll 1$. Then $z \simeq r_s + z_L$. If $s_0 = 50$ at some slotted-line reference plane when $z_L = 0$, then $r_s = 1/50$ giving 1 Ω in series with the load if $Z_0 = 50$ Ω. This is equivalent to a loss of only about 0.2 dB between the slotted-line reference plane and the load.

Variation of VSWR along Transmission-Line

Now, if $|\rho_L| = e^{-2\theta}$, then

$$s = \frac{1 + |\rho_L| e^{-2\alpha l}}{1 - |\rho_L| e^{-2\alpha l}} = \frac{1 + e^{-2(\theta + \alpha l)}}{1 - e^{-2(\theta + \alpha l)}} = \frac{1}{\tanh(\theta + \alpha l)}.$$

But

$$s_L = \frac{1 + e^{-2\theta}}{1 - e^{-2\theta}} = \frac{1}{\tanh \theta}.$$

Therefore,

$$\frac{1}{s} = \tanh \left\{ \tanh^{-1} \frac{1}{s_L} + \alpha l \right\}. \tag{9}$$

If $1/s_L \ll 1$ and $\alpha l \ll 1$,

$$\frac{1}{s} \simeq \frac{1}{s_L} + \alpha l \simeq \frac{1}{s_L} + \frac{1}{s_0}. \tag{10}$$

Equation (10) provides the basis of a first-order correction for VSWR for small attenuation. Greater accuracy is obtained by use of the exact equation (9).

III. Characterization of the Tunnel-Diode and its Mount

Reference Plane and Mount Equivalent Circuit

Some manufacturers quoting an "inductance" for their tunnel-diode actually imply an "excess inductance with respect to a conducting block of the same geometry" in a particular environment, e.g., coaxial-line or rectangular waveguide. (See Hauer[7] for an alternative definition based on the maximum frequency of oscillation.) Most authors rarely distinguish between these concepts, let alone discuss the implications of their choice of reference plane. Amplifier designers usually tailor the microwave environment around the tunnel-diode to minimize external parasitic effects. Thus the additional inductance, for example, due to the mount can be small. Very large excess inductance has been observed by Bandler[8] in accordance with Getsinger.[9]

It is important, however, to know the parameters independent of the mount. Getsinger[9] has fully discussed the reactive discontinuity effects due to the mounts of packaged diodes and the concept of the reference plane. He also suggested criteria under which simplification of the equivalent circuit may be possible. The reactances of Getsinger's Figs. 6 and 7 applicable here (Fig. 4) have been evaluated; a reasonable approximation is given by an L section having series inductance L_m and shunt capacitance C_m, as shown in Fig. 2. The plane to which all measurements should be referred is the end of the center conductor. Any error in the plane's location would manifest itself substantially as an error in the series inductance of the diode.

Only two sets of measurements are required to estimate L_m and C_m. A conducting pill of the same dimensions as the diode provides a short circuit at the "diode terminal surface," and its reactance at the reference plane leads to L_m. No diode[1] provides an open circuit whose susceptance at the reference plane leads approximately to C_m. (Any error in C_m can be detected as a change in the apparent C_1; this is discussed in the following section.)

[1] Here, a center rod without a central hole and an end plate without a recess (see Fig. 4) are required.

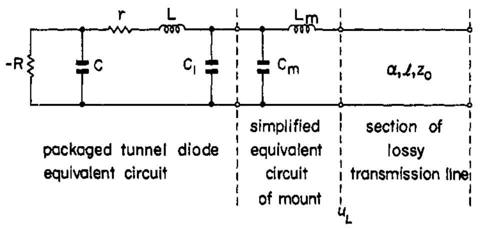

Fig. 2. Circuit representation of experimental setup.

Evaluation of the Internal Parasitics of the Tunnel-Diode

Fig. 2 shows the small-signal equivalent circuit of the tunnel-diode. R and C are the junction resistance and capacitance, respectively; r is the series resistance; L is the series inductance; and C_1 is the package capacitance. C, r, L, and C_1 are termed "parasitic"; C, r, and L will be termed "internal parasitics."

When biased at the valley voltage, the tunnel-diode exhibits $R=\infty$. The admittance Y_p of the remaining parasitic circuit is

$$Y_p = j\omega C_1 + \frac{1}{r + j\omega L + \dfrac{1}{j\omega C}} \cdot \tag{11}$$

Assume C_1 is known and removed from Y_p. The remaining circuit has impedance Z_s, given by

$$Z_s = r + \frac{1}{j\omega C}\left\{1 - \left(\frac{f}{f_0}\right)^2\right\} \tag{12}$$

where

$$f_0 = \frac{1}{2\pi\sqrt{LC}} \cdot \tag{13}$$

r can then be removed leaving X_s. An equivalent capacitance C_e can be defined by

$$\frac{1}{C_e} = \frac{1}{C}\left\{1 - \left(\frac{f}{f_0}\right)^2\right\} \cdot \tag{14}$$

Thus, if C_1 is correctly removed from the measured Y_p, followed by the removal of the real part of Z_s, a graph of $1/C_e$ against f^2 leads to $1/C$ at $f=0$, and hence, L from a knowledge of f_0. Note that no assumption concerning the frequency dependence of r is made, but C_1, C, and L need to be invariant for (14) to give a straight line. If C_1 is incorrectly chosen, the points will not lie on a straight line. Scanlan and Kodali[6] and Unotoro[8] concerned themselves with the conditions under which r or the VSWR, or both, could be neglected. This was not done here.

IV. Experiments

The diodes measured are Mullard types AEY13 to 16 germanium tunnel-diodes commonly employed in low-noise microwave amplifiers. See Fig. 3.

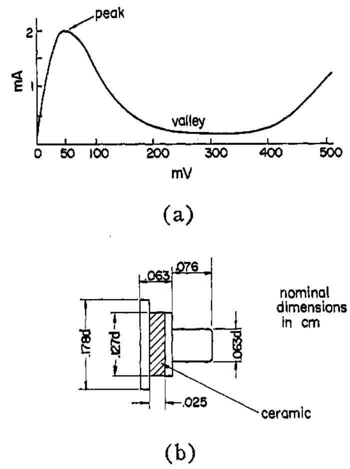

Fig. 3. The tunnel-diode used. (a) Typical dc characteristic. (b) Outline of its encapsulation.

The Apparatus

Fig. 4 shows the important parts of the 7 mm coaxial-line mount. It was machined in brass then silver plated and rhodium flashed. The diode is held by a coil spring and a sliding spring finger contact (the fingers ensuring electrical contact with the center rod at the diode). The springs are depicted as if the tunnel-diode were actually present. A thin dielectric sheet separates the end plate from the outer conductor of the coaxial-line so that dc bias can be applied. Fig. 5 is a photograph of the assembled mount. (The Precifix A sexless connector mates the mount with the slotted-line.) The apparatus is represented by Fig. 6. The slotted-line was a 50 Ω precision AMCI type 2920; the probe was untuned. The modulated microwave signal was applied to the probe. Every effort was made to receive the maximum power at the input to the balanced mixer. Thus the power at the tunnel-diode could be kept at the lowest level compatible with low-noise reception. The circulator minimized leakage of the LO signal to the slotted-line. It also retained the broadband dc return which linked the inner and outer conductors for biasing. The calibrated attenuator at the input to the IF amplifier was used with the audio amplifier's attenuator to indicate relative power levels.

The Measurement Technique

A digital computer processed the measurements. These were carried out in a sequence convenient to the operator, so that the results could be fed into the computer with a minimum of rearranging. An algorithm of the program is available.[10]

Fig. 7(a) illustrates the situation at the jth minimum (starting from the furthest from the load). The receiver attenuation was adjusted for a given deflection to be observed on the audio indicator. The attenuation was then increased by a prescribed amount p, and the carriage moved away from the minimum until the indicator returned to its value at the minimum. Let the dif-

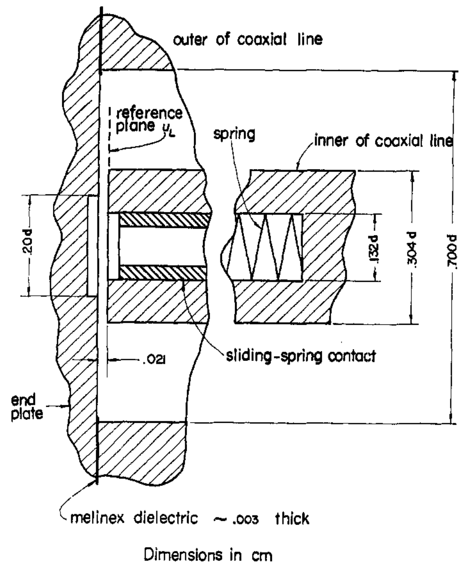

Fig. 4. Important details of the coaxial-line mount.

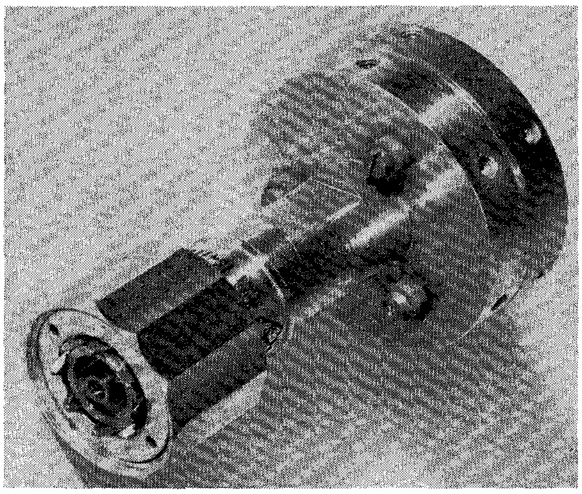

Fig. 5. The assembled mount.

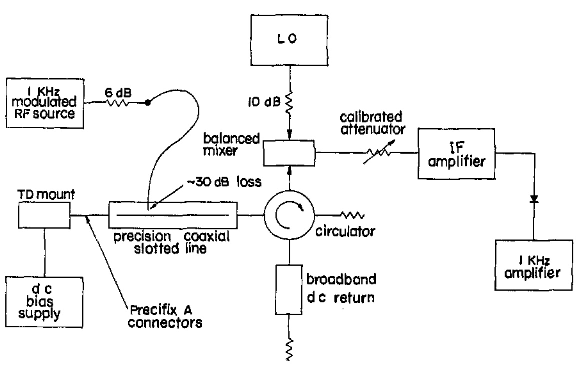

Fig. 6. The experimental setup for precision tunnel-diode measurements from 4 to 11 GHz.

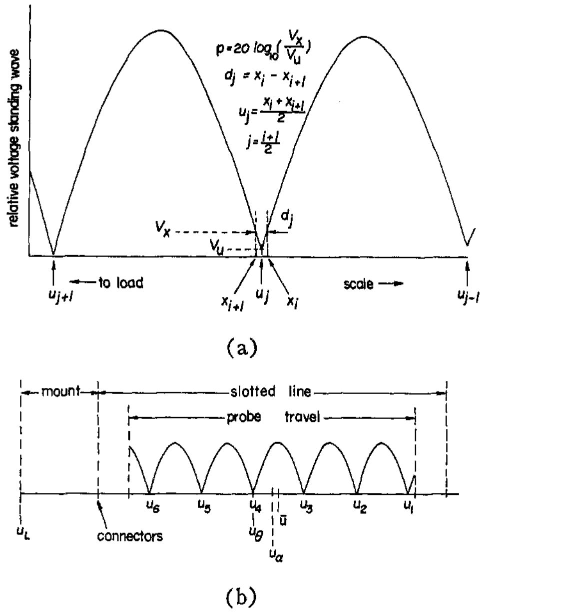

Fig. 7. Sketch of the standing wave showing (a) the detail at the jth minimum and (b) the case when $n=6$ and the location of the planes $\bar{u}$, u_α, u_θ, and u_L.

ference between this position x_i and the opposite one x_{i+1} be d_j. If the VSWR does not change appreciably over the range of d_j, we can assume[11]

$$s_j = \frac{\{\exp(0.23026p) - \cos^2(\pi d_j/\lambda_g)\}^{1/2}}{\sin(\pi d_j/\lambda_g)} \tag{15}$$

where λ_g is the wavelength in the slotted-line. This procedure was repeated at every minimum available, p being held constant. All readings of position and p were fed into the computer.

Note also that as $d \to 0$, $s \to k/d$, where k is a constant. Thus from (10), d would vary almost linearly along the slotted-line provided p was fixed. Hence, it seemed justifiable to define an average value of d as

$$\bar{d} = \frac{1}{n}\sum_{j=1}^{n} d_j \tag{16}$$

where n is the number of available minima, at the "average position" of the minima $\bar{u}$, where

$$\bar{u} = \frac{1}{n}\sum_{j=1}^{n} u_j \tag{17}$$

leading to an average VSWR $\bar{s}$ obtained from (15). Fig. 7(b) illustrates the case when $n=6$. λ_g was calculated as

$$\lambda_g = 2\frac{u_1 - u_n}{n-1}. \tag{18}$$

$\bar{s}$ was corrected for slotted-line attenuation A_{sl} dB/cm to a convenient point u_α, called the attenuation reference plane, about half way along the slotted-line by use of (10), giving

$$s_\alpha = \bar{s}\{1 + 0.1151\bar{s}A_{sl}(\bar{u} - u_\alpha)\}. \quad (19)$$

The remaining total attenuation A_T dB to the load was corrected for using (9), and giving

$$s_L = \coth\left\{\tanh^{-1}\frac{1}{s_\alpha} - 0.1151\, A_T\right\}. \quad (20)$$

The angle θ between a minimum at u_θ and the load reference plane u_L is[2]

$$\theta = 2\pi\frac{u_\theta - u_L}{\lambda_g}. \quad (21)$$

where [see Fig. 7(b)]

$$u_\theta = \begin{cases} \bar{u} & n \text{ odd} \\ \bar{u} - \dfrac{\lambda_g}{4} & n \text{ even.} \end{cases} \quad (22)$$

z_L is then given by the familiar

$$z_L = \frac{1 - js_L \tan\theta}{s_L - j\tan\theta}. \quad (23)$$

Calibration of the System

The load reference plane u_L was first found approximately. The center rod (Fig. 4) was replaced by a longer one which made firm contact with the end plate. The positions of standing-wave minima were determined at intervals of 1 GHz from 4 to 11 GHz. These positions were extrapolated graphically by integral numbers of half wavelengths until they coincided; hence, the location of the end plate. An instruction in the computer program bypassed the attenuation correction facility. The location of the end plate was then refined by trial and error by ensuring that the load reactance was as close as possible to zero from 4 to 11 GHz. The final value consistent with the slotted-line scale was -8.330 ± 0.002 cm. The scatter about zero was very small confirming that the system was substantially free from defects. Since the reference required was 0.021–0.003 cm from the end plate (the dielectric sheet was not present), $u_L = -8.312$ cm. Half the return loss at each frequency gave the attenuation from $\bar{u}$ to the end plate. The experimental results were then fed back into the computer as follows. The readings of position at each frequency were separated into two sets, one for each half of the slotted-line. Each set was processed separately. A_{sl} was calculated from the *difference* in return loss and "average positions" of the corresponding sets. u_α was chosen to be 12.0 cm. The total attenuation at each frequency was transformed to u_α to give A_T, by adding or subtracting $(\bar{u} - u_\alpha)A_{sl}$.

Fig. 8(a) records the results for attenuation. Note that A_{sl} happens to be consistent with the total attenuation A_T. Finally, the configuration of Fig. 4 was assembled. The reactance due to L_m and susceptance due to C_m versus frequency are shown in Fig. 8(b). In the former experiment two tunnel-diode shaped pills were available, one plain brass and the other silver plated.

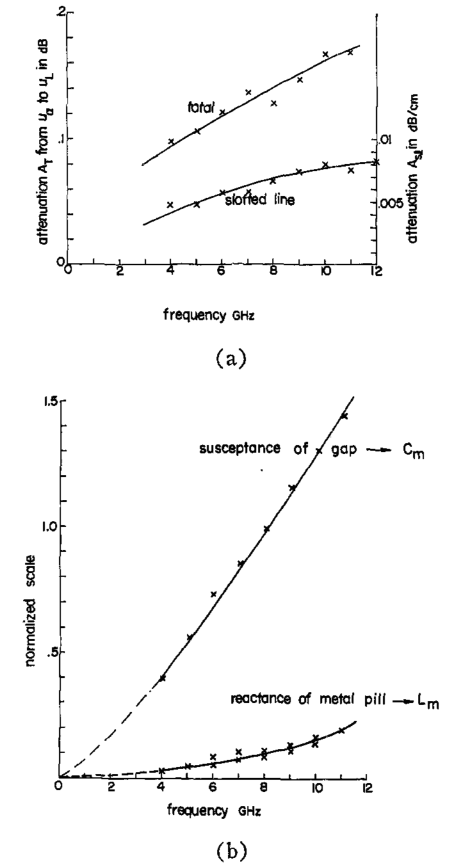

Fig. 8. (a) Attenuation of the transmission-line. (b) Discontinuities between the reference plane and the tunnel-diode.

The Results

The results for a particular tunnel-diode (TD1) are plotted in Fig. 9. Several points at one frequency indicate that the measurement was repeated at different power levels to show up any nonlinear effects. At 6 GHz, for example, the power ranged over 40 dB. p was generally 10 dB, occasionally 20 dB. The straightest line of $1/C_e$ against f^2 emerged when C_1 was taken as zero. This is reasonable since the full quoted value is only 0.3 pF and the tunnel-diode package forms part of the mount. Experimentally, C_m was probably slightly overcompensated for, due to the assumption that no diode was equivalent to an open circuit. Since it was observed that the series resistance tended to increase quadratically with frequency, a least-squares fit of a curve of this type to the experimental points was made.[3] The same technique was used to determine the best straight line

[2] To reduce θ to its equivalent between $-\pi/2$ and $\pi/2$ for tangent calculations, set θ equal to $\theta - \pi \times$ integral part of $(0.5 + \theta/\pi)$.

[3] A least-squares fit eliminated any further subjective analysis of the measurements.

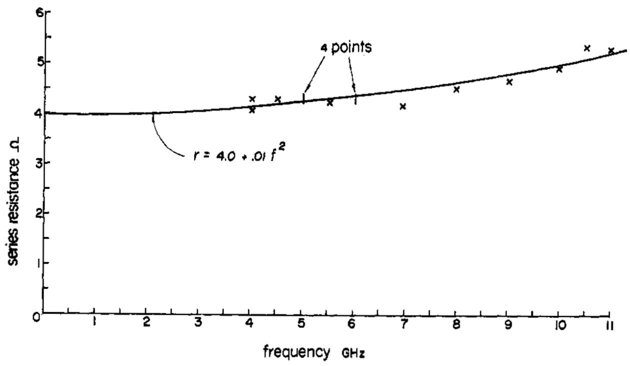

(a)

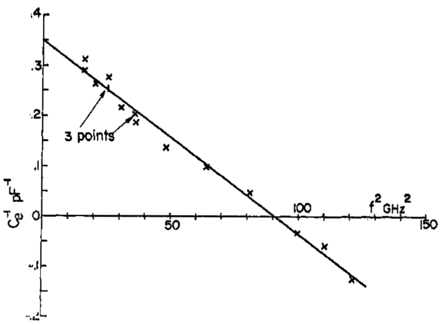

(b)

Fig. 9. Experimental results for TD1. (a) Series resistance against frequency. (b) C_e^{-1} against f^2.

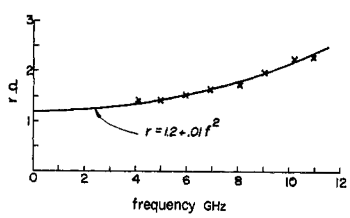

(a)

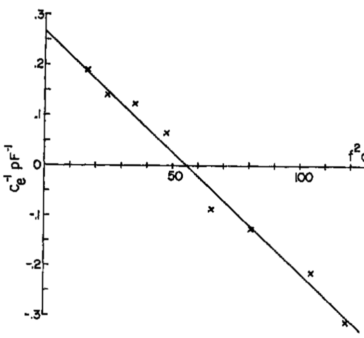

(b)

Fig. 10. Experimental results for TD2. (a) Series resistance against frequency. (b) C_e^{-1} against f^2.

TABLE I

Summary of Measured Results on Four Tunnel-Diodes, and Comparison with the Manufacturer's Quoted Values*†

	Microwave Measurements				Manufacturer's Values		
	L (nH)	C (pF)	r_{dc} (Ω)	a^2 (Ω/GHz²)	L (nH)	C (pF)	r (Ω)
TD 1	0.10	2.86	3.96	0.0104		2.9	~4
TD 2	0.12	3.73	1.20	0.0096	0.12	3.9	1.2
TD 3	0.12	3.96	1.45	0.0095		4.0	1.8
TD 4	0.11	0.73	4.05	0.0094		0.7	~4

* Assumed value of L for TD4.

† r and C were measured by the manufacturer at substantially zero frequency; r by a large bias current method, C at the valley voltage at 300 kHz and 4 MHz. L was obtained from microwave measurements on dummy diode packages. The peak currents for TD1 to TD4 are 2.1, 2.1, 2.2, and 1.9 mA.

for the points for $1/C_e$ against f^2. Fig. 10 records the results for TD2. These and the results for two more diodes are summarized in Table I. In all instances $r = r_{dc} + (af)^2$ to a very good approximation, r_{dc} and a being constants. It is interesting that $a = 0.1$ within experimental error, and seems independent of r_{dc} and the junction parameters.

V. Discussion

Resistive Cutoff Frequency

At the resistive cutoff frequency ω_R, the equivalent series resistance of the tunnel-diode vanishes. If

$$r = r_{dc} + (A\omega)^2 \tag{24}$$

then

$$r_{dc} + (A\omega_R)^2 + \frac{-G}{G^2 + (\omega_R C)^2} = 0 \tag{25}$$

where A is constant and $G = 1/R$. After some manipulation,

$$\frac{\omega_R^4}{\dfrac{r_{dc}}{A^2} + \left(\dfrac{G}{C}\right)^2} + \omega_R^2 - \frac{\omega_{R0}^2 \dfrac{r_{dc}}{A^2}}{\dfrac{r_{dc}}{A^2} + \left(\dfrac{G}{C}\right)^2} = 0 \tag{26}$$

where

$$\omega_{R0}^2 = \left(\frac{G}{C}\right)^2 \left(\frac{1}{r_{dc}G} - 1\right). \tag{27}$$

Note that ω_{R0} is the conventional resistive cutoff frequency based on $r = r_{dc}$. The solution of interest is given by

$$\omega_R^2 = \frac{\left[\dfrac{4\omega_{R0}^2 \cdot \dfrac{r_{dc}}{A^2}}{\left\{\dfrac{r_{dc}}{A^2} + \left(\dfrac{G}{C}\right)^2\right\}^2} + 1\right]^{1/2} - 1}{\dfrac{2}{\dfrac{r_{dc}}{A^2} + \left(\dfrac{G}{C}\right)^2}}. \quad (28)$$

This is the only solution for which ω_R is real, with the proviso that $\omega_{R0}^2 > 0$ must hold for a useful microwave tunnel-diode. If $A \rightarrow 0$, then by applying the binomial expansion to the expression under the square root, it can be shown that $\omega_R^2 \rightarrow \omega_{R0}^2$. In general, however, $\omega_R < \omega_{R0}$.

Table II shows the maximum resistive cutoff frequencies of TD1 and TD2. Note that C is corrected for variation with bias voltage,[4] and $R_{\min}$ is the minimum value of R. (There is no dispute among the main authors of tunnel-diode measurement papers concerning the variation of C with bias, or the fact that the R does not vary with frequency.)

Comparison with the Results of Other Researchers

Three papers which consider the variation of series resistance with frequency[1],[4],[6] will be discussed. Fig. 11(a), (b), and(c) reproduces the results published by Fukui,[1] Kim and Lee,[4] and Scanlan and Kodali,[6] respectively. The curves drawn are the best quadratic approximations. The scatter of the points about the curves could reasonably be due to experimental error. Fukui proposed an equation of the form

$$r = r_{dc} + k\sqrt{f} \quad (29)$$

which appears to have been adopted without much further research,[2],[3] partly because of the difficulty in isolating the series resistance from the measurements with sufficient accuracy.[12] This equation implies that the greatest change in r occurs at dc. Fig. 11(b) and (c), and the experiments of Hawkins,[13] however, support the contention that $dr/d\omega = 0$ at dc.

Scanlan and Kodali claim that

$$r = r_{dc} + K(f - f_c)\begin{cases} K = 0 & f < f_c \\ K > 0 & f > f_c \end{cases} \quad (30)$$

where K and f_c are constants. This variation suffers from an improbable discontinuity at f_c. It is a good approximation to their experimental points, but Scanlan and Kodali's theoretical justification for (30) is questionable.

The quadratic approximation to r proposed here is not inconsistent with skin effect in circular conductors[14] for

[4] C at $R_{\min}$ was calculated from

$$C_{\text{valley}}\sqrt{(580 - V_{\text{valley}})/(580 - 95)}$$

where 580 is the built-in potential of the junction, and 95 is the voltage at $R_{\min}$, both in mV. V_{valley} for TD1 was 360 mV, for TD2 it was 330 mV.

TABLE II
COMPARISON OF RESISTIVE CUTOFF FREQUENCIES FOR TD1 AND TD2

	$R_{\min}$ (Ω)	C at $R_{\min}$ (pF)	f_{R0} (GHz)	f_R (GHz)
TD 1	50	1.9	5.7	5.5
TD 2	50	2.7	7.5	6.4

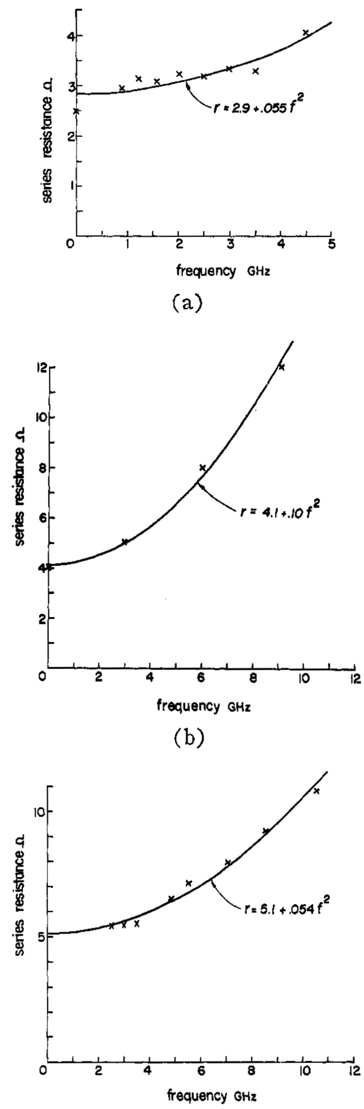

Fig. 11. Series resistance against frequency of the experimental tunnel-diodes of other researchers. (a) Fukui.[1] (b) Kim and Lee.[4] (c) Scanlan and Kodali.[6]

which the $\sqrt{f}$ variation is a "high" frequency approximation, but where the "low" frequency approximation is of the form $r = r_{dc} + (af)^2$, the error increasing with f. Further study would, however, be necessary to establish theoretically the variation of r (see, for example, Dickens[15]) and to locate its origin. For the present these questions will be left open.

VI. Conclusions

Precise microwave standing-wave measurements have been carried out on four tunnel-diodes. The frequency invariance of the series inductance and junction capacitance has been verified, and agreement with the manufacturer's values is good. A new variation of series resistance with frequency has been proposed which seems also to represent very closely the relevant results of other researchers. A formula for resistive cutoff frequency has been derived incorporating this variation and assuming the junction negative resistance to be constant with frequency.

Acknowledgment

The author is pleased to acknowledge the cooperation of M. D. Coleman and J. F. Wells of Mullard Research Laboratories, Redhill, Surrey, England, who assisted with the measurements. Valuable discussions with J. F Wells are also gratefully acknowledged. M. K. McPhun, now with Warwick University, England, was responsible for the basic design of the mount.

References

[1] H. Fukui, "The characteristics of Esaki diodes at microwave frequencies," *1961 Internat'l Solid-State Circuits Conf., Digest of Technical Papers*, pp. 16–17.
[2] T. Unotoro and H. Niizuma, "Measurement of Esaki diodes," *Electronics and Commun.* (Japan), vol. 47, pp. 57–74, April 1964.
[3] T. Unotoro, "Microwave measurement of Esaki diode circuit parameters," *Electronics and Commun.* (Japan), vol. 47, pp. 64–71, May 1964.
[4] C. S. Kim and C. W. Lee, "Microwave measurement of tunnel-diodes," *Microwaves*, vol. 3, pp. 18–21, November 1964.
[5] P. Hawkins and M. K. McPhun, "The equivalent circuit of the tunnel-diode," *Proc. IEEE*, vol. 54, pp. 1451–1452, October 1966.
[6] J. O. Scanlan and V. P. Kodali, "Characterisation of tunnel diodes at microwave frequencies," *Proc. IEE* (London), vol. 114, pp. 1231–1236, September 1967.
[7] W. B. Hauer, "Definition and determination of the series inductance of tunnel diodes," *IRE Trans. Electon Devices*, vol. ED-8, pp. 470–475, November 1961.
[8] J. W. Bandler, "Stable broadband tunnel-diode amplifiers in rectangular waveguides," Ph.D. thesis, University of London, England, 1967.
[9] W. J. Getsinger, "The packaged and mounted diode as a microwave circuit," *IEEE Trans. Microwave Theory and Techniques*, vol. MTT-14, pp. 58–69, February 1966.
[10] J. W. Bandler, "Precision microwave measurement of the internal parasitics of tunnel-diodes," Mullard Research Laboratories, Redhill, Surrey, England, Rept. 580, July 1967.
[11] A. B. Giordano, "Measurement of standing wave ratio," in *Handbook of Microwave Measurements*, 3rd ed., vol. 1, M. Sucher and J. Fox, Eds. New York: Wiley, 1963, ch. 2.
[12] T. Unotoro, Electrical Communication Laboratory, Nippon Telegraph and Telephone Public Corporation, Musasino-si, Tokyo, Japan, private communication.
[13] P. Hawkins, Central Electricity Research Laboratories, Leatherhead, Surrey, England, private communication.
[14] S. Ramo, J. R. Whinnery, and T. van Duzer, *Fields and Waves in Communication Electronics.* New York: Wiley, 1965, pp. 286–303.
[15] L. E. Dickens, "Spreading resistance as a function of frequency," *IEEE Trans. Microwave Theory and Techniques*, vol. MTT-15, pp. 101–109, February 1967.

An Improved Dispersion Relationship for the *p–n* Junction Avalanche Diode

FRED K. MANASSE, MEMBER, IEEE, AND JONATHAN S. SHAPIRO, STUDENT MEMBER, IEEE

***Abstract*—A tractable and more physically realistic dispersion relationship for the avalanche diode than previously available has been developed. This includes terms relating to the differences in hole and electron velocities and ionization coefficients. Analysis of this modified dispersion relation indicates new ranges for instabilities. Plots for selected cases are presented.**

I. Introduction

THE small-signal analysis of the space-charge region of a *p–n* junction biased to avalanche breakdown, as developed by Misawa,[1] is useful for demonstrating that negative resistance can occur. The key to understanding the analysis lies in the dispersion relation for an applied plane space-charge wave which indicates that an instability can occur. The simplified analysis of Misawa assumed equal ionization rates for holes and electrons, as well as identical saturated drift velocities. While these assumptions were made in order to obtain a tractable equation, they mask certain aspects of the dispersion relation which may give rise to new instabilities. In a companion paper,[2] Misawa develops a rather elaborate computer solution which tends to complicate a more general interpretation of the results.

Manuscript received April 17, 1967; revised February 7, 1968.
The authors are with the School of Engineering and Applied Science, Princeton University, Princeton, N. J.